



Patient specific instrumentation for corrective osteotomy in case of posttraumatic cubitus varus in children

Nicolas F. BARBIER, Solange DE WOUTERS, Sidi Yaya TRAORE, Khanh TRAN DUY, Pierre-Louis DOCQUIER

From the Université catholique de Louvain, Secteur des Sciences de la Santé, Institut de Recherche Expérimentale et Clinique, Neuro Musculo Skeletal Lab (NMSK), Brussels, Belgium

Malunion in cubitus varus most often results from inadequate supracondylar fracture reduction or from secondary displacement. Treatment of cubitus varus needs an accurate preoperative planning to obtain a good functional and esthetical outcome. Planning based on conventional radiology is source of inaccuracy and clinical results are variable. Developments of computer-assisted orthopaedic surgery (CAOS) and of patient specific instruments (PSI) have made accurate three dimensional (3D) preoperative simulation possible. This original technique based on 3D-osteotomy planning and using PSI was developed to correct cubitus varus deformity in the three dimensions.

A 3D-model of the deformity was created based on a CT-scan of the distal humerus. Ideal correction was calculated by software and a PSI was designed. The PSI was used to guide the saw blade on the deformed bone. After resection of a wedge fragment, osteosynthesis was performed using two crossed K-wires. Elbow radiographs were performed at least six months after surgery.

At the latest follow-up, the correction of cubitus varus obtained was satisfying in the five cases of our series and all the patients had pain free elbow mobility.

Ulnar nerve palsy complicated the evolution in one patient, which fully recovered within 6 months.

Advantages of this technique include a decreased operating time and a smaller surgical incision. Moreover, results showed increased correction accuracy without the need of fluoroscopy during the osteotomy procedure. These benefits are counterbalanced by the

need of a preoperative CT-scan of the distal humerus and the additional cost for the PSI.

Keywords : Cubitus varus ; tridimensional planning ; humerus osteotomy ; children ; supracondylar fracture.

INTRODUCTION

Supracondylar fracture of the humerus is the most common paediatric elbow fracture. The peak age of presentation is 5 to 6 years old and the left and non-dominant arm is more frequently involved (19). It represents about 17% of all fractures in paediatric patients (11), resulting often from a fall from a height during sport and leisure activities (10). Malunion in

- Nicolas F. Barbier^{1,2}, MD
- Solange De Wouters^{1,2}, MD
- Sidi Yaya Traore^{1,2}, MD
- Khanh Tran Duy³, PhD,
- Pierre-Louis Docquier^{1,2}, MD, PhD

¹Université catholique de Louvain, Secteur des Sciences de la Santé, Institut de Recherche Expérimentale et Clinique, Neuro Musculo Skeletal Lab (NMSK), Brussels, Belgium.

²Cliniques universitaires Saint-Luc, Service de Chirurgie orthopédique et Traumatologique, Brussels, Belgium.

³3D-Side, patient specific surgical technology, Louvain-la-Neuve, Belgium.

Correspondence: Nicolas BARBIER, Cliniques Universitaires Saint-Luc, Service de Chirurgie Orthopédique et Traumatologique, Avenue Hippocrate, 10, B-1200 Brussels, Belgium.

E-mail : nicolas.barbier@uclouvain.be

© 2019, Acta Orthopædica Belgica.

Conflict of interest : the authors declare that they have no conflict of interest apart from Khan Tran Duy who could have as a co-founder of 3D-side.

cubitus varus may occur from inadequate fracture reduction (medial rotation of the distal fragment) (15). Growth disturbance of the humerus after fracture is uncommon. Cubitus varus does not impair elbow function or elbow range of motion in most of the cases, but the cosmetic deformity may lead parents to ask for an operation to improve the appearance of the elbow (1,12,15,22). An increased risk of lateral condylar fracture, ulnar nerve dislocation, triceps snapping, posterolateral rotary instability of the elbow, and posterior shoulder instability are rare sequelae of cubitus varus that have been reported in the literature (5, 9).

Treatment of cubitus varus is a challenge for the orthopaedic surgeon. Several surgical techniques have been reported including simple lateral closing-wedge osteotomy (1,15), anterolaterally based closing-wedge osteotomy (14,23) and three-dimensional (3D) corrective osteotomy (4,7,13,22,25). However, 3D-osteotomy planning is complicated and the rotational correction renders internal rigid fixation more difficult due to the relatively small contact area at the osteotomy site (20).

In the literature, surgical correction of post-traumatic cubitus varus has a high rate of complications and a variable clinical result. Complications include nerve damage, failure of fixation, deformity recurrence, under- or overcorrection,

lateral condylar prominence, patient dissatisfaction with residual scar and loss of motion. Parents should be informed about these potential complications. The posterior approach has also been related to increased incidence of nerve palsies versus none with lateral triceps-sparing approach (16).

Anatomically accurate correction is the key to obtain a good functional and esthetical outcome (6,17), but it needs an accurate preoperative planning. Planning based on conventional radiology may be source of inaccuracy because of important errors in the angular measurements (1,24).

With the developments of computer-assisted orthopaedic surgery (CAOS) and of patient specific instruments (PSI), the trend in medical technology has been toward individualization which has made accurate 3D preoperative simulation possible (2). A significant improvement in cutting accuracy can be achieved with these technologies (3). We describe a new technique using PSI and osteotomy fixation with K-wires.

MATERIALS AND METHODS

Patient series

Five patients underwent cubitus varus surgical correction with the use of a PSI. Preoperative

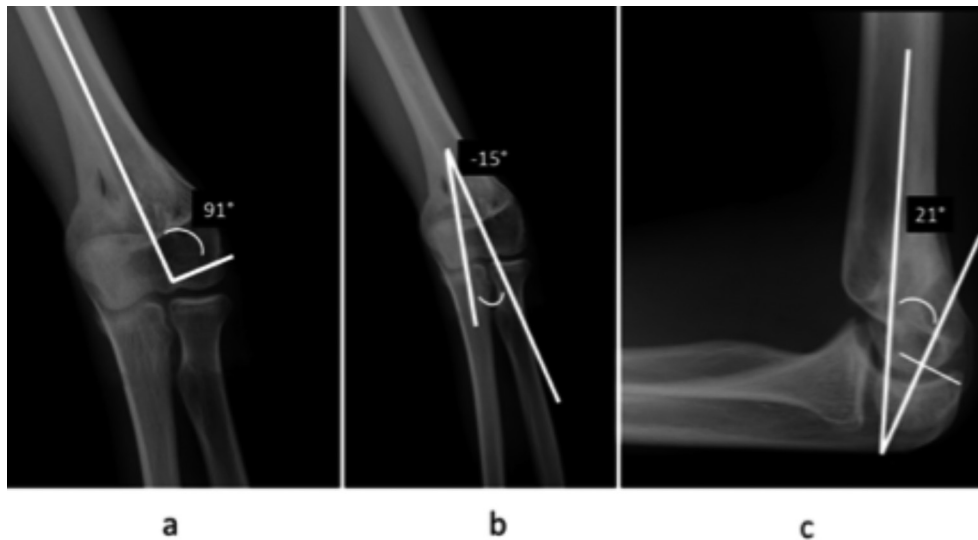


Fig. 1. — Radiographic angles measurement on a left elbow showing cubitus varus deformity : **a** radiographic Baumann's angle measurement on AP view ; **b** radiographic carrying angle measurement on AP view ; **c** radiographic humero-condylar angle measurement on lateral view.

3D-planning was based on a CT-scan of the humerus. All cubitus varus deformities resulted from a malunion after a supra-condylar fracture. Table I summarizes clinical and radiological data of the patients included in this study. The mean age was 10.2 years old (range 4-15 years) at the time of surgery. All procedures were performed in accordance with the ethical standards of the institutional research committee. An informed consent was obtained from all individual participants included in this study.

Radiographic Baumann's angle measurement

On the antero-posterior (AP) view of the elbow, a line was drawn along the long axis of the humerus and another through the physis of the lateral condyle of the distal humerus. The angle between these two lines corresponds to the Baumann's angle (Fig. 1-a).

Radiographic carrying angle measurement

On the AP view, two mid-points were identified at the level of the radial tuberosity and at the most proximal ossification point of the ulna and two others corresponding to the level of the mid diaphysis and mid distal metaphysis of the distal humerus. The carrying angle is given by the intersection of two lines drawn through these points (21) (Fig.1-b).

Radiographic humero-condylar angle measurement

On the lateral view of the elbow, a line was drawn along the long axis of the distal humerus shaft and another along the axis of the distal humeral condyle. The angle between these two lines is defined as the humero-condylar angle, also called shaft-condylar angle (Fig.1-c).

Determination of the ideal correction and osteotomy principles

The ideal correction, planned in three dimensions was based on the combination of a correction in the frontal plane and a correction in the sagittal plane. Additionally, this technique allows correction of the unsightly lateral bump of the lateral condyle. The

osteotomy cannot always be done at the site of the previous fracture and sometimes a former collapse of the medial pillar is present. Due to interindividual differences, the correction in the frontal plane was based on the difference of the humerus elbow-wrist angle (12,20) between the normal side and the deformed side measured clinically by goniometry. This clinical measure seemed important because of the essentially aesthetic purpose of this operation and because of the need to obtain symmetry. The humerus-elbow-wrist angle is related to the carrying angle measured on radiographs and reported in Table I. The correction in the sagittal plane was calculated on the pre-operative CT to restore a normal humeral-condylar angle, close to 40° (normal range 30 to 70° (18) Simanovsky, 2008 #367).

Preoperative 3D-planning for osteotomy

A preoperative humerus CT-scan with 2-mm slice thickness and 1-mm spacing between slices was performed using a Brilliance 40 CT-scanner (Philips, the Netherlands). Varus and flexion or extension deformities were assessed on a 3D-reconstruction of the distal humerus obtained with Mimics software (Materialise, Leuven, Belgium). The closing wedge was planned proximally to the olecranon fossa to correct the frontal, sagittal and rotatory plane. No hinge was left at the opposite side to allow medial translation of the distal fragment and to decrease the residual condylar prominence.

PSI production

The PSI as well as a model of the patient's humerus were designed based on the 3D computer simulation (Fig. 2) and were manufactured using polyamide biocompatible material by selective laser sintering (rapid manufacturing technology) (2).

The PSI consisted of two different parts :

- A first main PSI designed to place 4 K-wires in the humerus and used as cutting guide (Fig. 3-a).
- A second external fixator (Fig. 3-b) which imposes the final position but with a freedom in translation (Fig. 3-c).

The 2 parts of the PSI were sterilised and were available during the surgery.

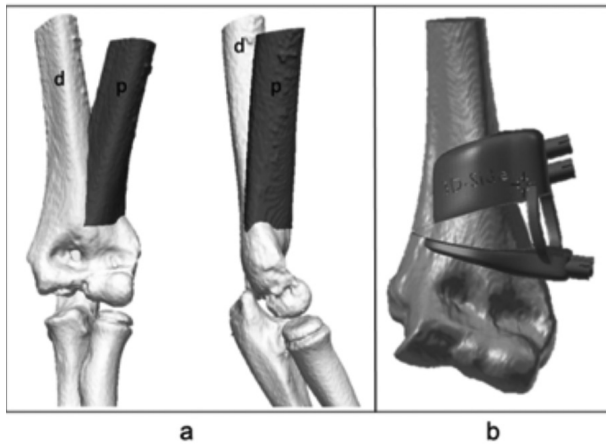


Fig. 2. — Elbow with cubitus varus deformity : **a** frontal and lateral views of the deformed (d) humerus and of the humerus after multiplanar (p) correction by closing wedge osteotomy ; **b** the PSI was designed based on 3D computer simulation.

Corrective osteotomy using PSI

A model of the deformed humerus was available to help the surgeon during the surgery. While the patient was in the supine position, the deformed arm was installed on an arm board and a tourniquet was placed at the basis of the limb. A lateral approach was used. After a 5cm skin incision, soft-tissues were carefully dissected until the periosteum. The distal humeral metaphysis was exposed by opening longitudinally the periosteum. The PSI was placed proximally to the olecranon fossa and displaced until it fits perfectly to the bone (Fig. 4-a). Four 2mm-K-wires were inserted in the distal humerus by following the PSI. The PSI was separated in two parts by removal of the junction bridges (Fig

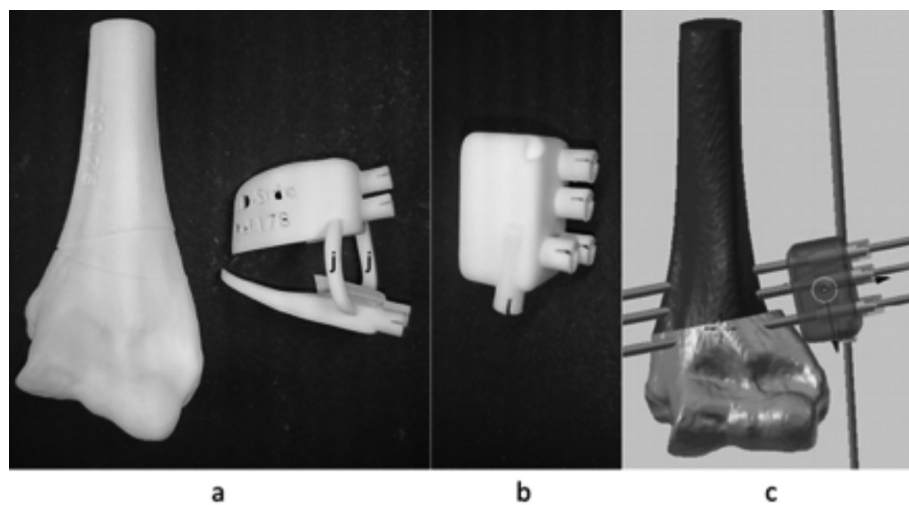


Fig. 3. — The PSI was made of 2 different parts : **a** The main part was designed to receive 4 K-wires and was used as cutting guide after resection of the 2 junction bridges (j) ; **b** The second PSI was used as an external fixator which imposed the final correction (closing wedge) ; **c** Translation was free through the second PSI in order to decrease the residual condylar prominence.

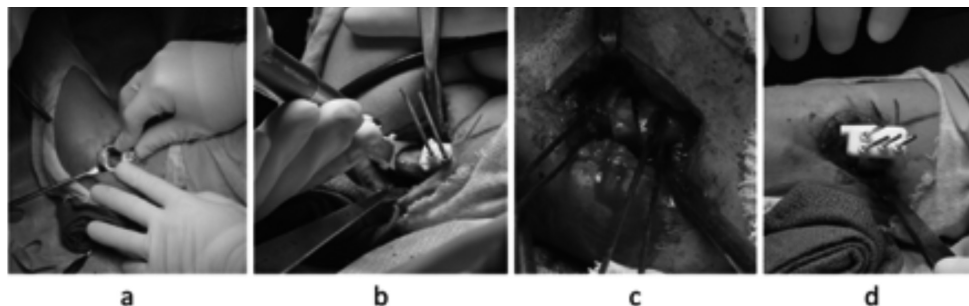


Fig. 4. — **a** The PSI was displaced until the unique position was reached ; **b** Four 2mm-K-wires were inserted in the distal humerus by following the PSI which also served as cutting guide after division of the 2 union bridges ; **c** The wedge fragment was removed ; **d** The planned correction was directly obtained by placing the four K-wires in a second guide used as a temporary external fixator.

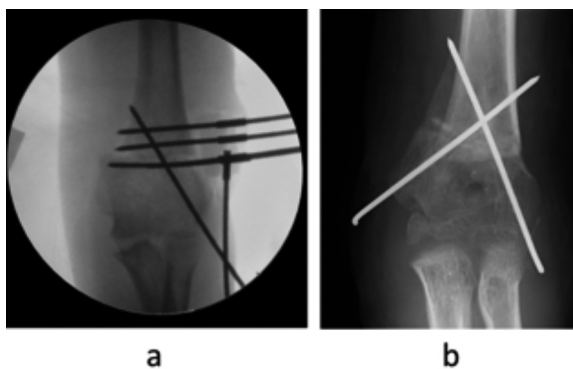


Fig. 5. — **a** Perioperative fluoroscopy of the elbow to control the placement of the 2 mm K-wire crossing the osteotomy line after the closing wedge resection ; **b** Postoperative radiograph at three weeks showing the final osteosynthesis with two crossed K-wires and good bone healing.



Fig. 6. — **a** Preoperative antero-posterior radiograph of an elbow with cubitus varus deformity ; **b** The same elbow corrected by the previously described technique at 6 months after surgery.

3-a) and a lateral closing wedge osteotomy was performed with the oscillating saw by following the cutting guide (Fig. 4-b). No hinge was left at the opposite side. The wedge fragment was removed (Fig. 4-c).

The two humeral parts were finally joined as planned by placing the four K-wires in the second PSI used as a temporary external fixator (Fig. 4-d ; Fig. 5-a). Lateral translation was performed

to correct the lateral condylar prominence. Final osteosynthesis was obtained by two crossed 2mm-K-wires (Fig. 5-b). The four initial K-wires were then removed.

Post-operative period

After surgery, all patients were immobilized with the arm flexed at 90° in a long-arm posterior splint for three weeks without change. At 3 postoperative weeks, osteotomy consolidation was obtained on radiographs and the K-wires were removed. Active elbow mobilisation was allowed after three weeks and sports were allowed after three months. Patients were followed at least during six months after surgery. Baumann's angle, carrying angle and humero-condylar angle were measured at last follow-up. No additional postoperative CT-scan was performed according to radioprotection rules.

RESULTS

Table I summarizes postoperative osteotomy results for the five children.

At 3 weeks postoperatively, radiographs showed bone healing in all cases and K-wires were removed. Final evaluation was performed on radiographs at 6 months postoperatively (Fig.6).

Cubitus varus rectification was satisfying for the five patients at 6 months postoperatively. Comparison at 6 months postoperatively between planned and measured carrying angles showed errors of 0°, 4°, 1°, 1° and 7° respectively (Table I).

The mean post-operative radiographic carrying angle was +8° (range -5° to +20°). The mean post-operative Baumann's angle was 65° (range 51° to 75°) and the mean humerocondylar angle was 47° (range 35° to 62°). An ulnar nerve palsy (confirmed by electromyography) complicated the evolution of one patient (case 4). A spontaneous recovery was noted without sequelae at 6 months.

In all cases pain was controlled in the postoperative period with step 1 analgesics. A full and pain free elbow mobility was noted in all patients at the latest follow-up.

Table I. — Clinical and radiological data of the patients included in the study

Case	Sex	Age at time of surgery (years)	Origin of cubitus varus	Baumann's angle		Radiographic carrying angle			Humero-condylar angle	
				Pre-operative value	Post-operative value (latest follow-up)	Pre-operative value	Planned resected angle	Post-operative value (latest follow-up)	Pre-operative value	Post-operative value (latest follow-up)
1	F	10	Supracondylar fracture at the age of 6.5 years	+89°	+67°	-16°	+26°	+10°	+29°	+35°
2	M	15	Supracondylar fracture at the age of 13 years	+91°	+75°	-16°	+15°	-5°	+2°	+42°
3	M	10	Supracondylar fracture at the age of 6 years	+60°	+51°	-10°	+21°	+12°	+32°	+45°
4	F	11	Supracondylar fracture at the age of 3 years	+78°	+71°	-6°	+25°	+20°	+31°	+62°
5	F	11	Supracondylar fracture at the age of 3 years	+69°	+62°	-10°	+22°	+5°	+30°	+50°

DISCUSSION

For an accurate correction of a cubitus varus, the deformity has to be considered in the three planes to obtain good results in terms of appearance and function (20). In previous studies, corrective osteotomies were mostly planned on basis of frontal and sagittal radiographs. However, finding the optimal saw blade orientation in the 3 dimensions preoperatively is very difficult. Moreover, extensive surgical exposure of distal humerus is necessary for most of previously described osteotomy techniques. Planning based on 3D-imaging is one way to improve the corrective osteotomy accuracy.

With this original technique, the deformity is accurately analysed in 3D during the preoperative planning. The PSI is designed specifically for the patient to fit its deformed humerus. It is placed proximally to the olecranon fossa and displaced until the unique position is reached. Surgical time is decreased by this technique as no measurement is needed during surgery : the PSI guide gives the planned angle for wedge resection without fluoroscopic guidance.

The need of a preoperative CT-scan exposing patient to radiations and the supplemental financial

cost for the patient are disadvantages of the technique.

Zhang et al. (26) reported also the correction of cubitus varus by rapid prototyping guide using 3D CT-Scan for the preoperative planning. However, they did not consider the medial translation and did not attempt to decrease the residual condylar prominence (26). On the contrary, the technique described in the present study allows a lateral translation of the proximal part after the wedge fragment resection. Takeyasu et al. (20) used a similar technique with 3D CT-planning and PSI but the final osteosynthesis was performed with screwed plates. With the crossed wires technique, no further surgery is needed to remove the plate as the wires are removed in the outpatient clinic without general anaesthesia.

Other studies have shown the accuracy of PSI. In the study of Zhang et al (26), the mean postoperative carrying angle in 18 patients was 7.3° (range, 5° to 11°). In the study of Takeyasu et al. (20), the mean differences in the carrying angle between the affected and normal sides improved from 25.3° preoperatively to 1.3°±3° postoperatively.

Without using 3D planning and PSI, Bellemore et al. (1) obtained correction with differences in the

carrying angle between affected and normal sides of less than 5° in only 20 patients out of 27 (74%).

Gong et al. (8) used an oblique osteotomy, plate osteosynthesis and preoperative planning based on radiographs. They hypothesized that oblique osteotomy gives a more important contact surface between the fragments favouring bone healing in a series of adult patients. In our paediatric patients, no healing delay was observed with a horizontal osteotomy.

Further improvements of our technique could include the use of a medial approach for its cosmetic advantage.

Ethical approval

All procedures performed in studies involving human participants were in accordance with the ethical standards of the institutional and/or national research committee and with the 1964 Helsinki declaration and its later amendments or comparable ethical standards.

REFERENCES

1. **Bellemore MC, Barrett IR, Middleton RW, Scougall JS, Whiteway DW.** Supracondylar osteotomy of the humerus for correction of cubitus varus. *J Bone Joint Surg* 1984 ; 66-B : 566-72.
2. **Brown GA, Firoozbakhsh K, DeCoster TA, Reyna JR, Jr., Moneim M.** Rapid prototyping : the future of trauma surgery? *J Bone Joint Surg* 2003 ; 85-A Suppl 4 : 49-55.
3. **Cartiaux O, Paul L, Docquier PL, Raucent B, Dombre E, Banse X.** Computer-assisted and robot-assisted technologies to improve bone-cutting accuracy when integrated with a freehand process using an oscillating saw. *J Bone Joint Surg* 2010 ; 92-A : 2076-82.
4. **Chung MS, Baek GH.** Three-dimensional corrective osteotomy for cubitus varus in adults. *J Shoulder Elbow Surg* 2003 ; 12 : 472-5.
5. **Davids JR, Maguire MF, Mubarak SJ, Wenger DR.** Lateral condylar fracture of the humerus following posttraumatic cubitus varus. *J Pediatr Orthop* 1994 ; 14 : 466-70.
6. **Fernandez DL.** Malunion of the distal radius : current approach to management. *Instr Course Lect* 1993 ; 42 : 99-113.
7. **French PR.** Varus deformity of the elbow following supracondylar fractures of the humerus in children. *Lancet* 1959 ; 2 : 439-41.
8. **Gong HS, Chung MS, Oh JH, Cho HE, Baek GH.** Oblique closing wedge osteotomy and lateral plating for cubitus varus in adults. *Clin Orthop Relat Res* 2008 ; 466 : 899-906.
9. **Gurkan I, Bayrakci K, Tasbas B, Daglar B, Gunel U, Ucaner A.** Posterior instability of the shoulder after supracondylar fractures recovered with cubitus varus deformity. *J Pediatric Orthop* 2002 ; 22 : 198-202.
10. **Houshian S, Mehdi B, Larsen MS.** The epidemiology of elbow fracture in children : analysis of 355 fractures, with special reference to supracondylar humerus fractures. *J Orthop Sci* 2001 ; 6 : 312-5.
11. **Khan MA, Khan A, Hakeem A, Askar Z, Durrani N, Durrani MZ, et al.** Results of type-III supracondylar fracture humerus with open reduction and internal fixation in children after failed closed reduction. *J Ayub Med Coll Abbottabad* 2010 ; 22 : 35-6.
12. **Kim HT, Lee JS, Yoo CI.** Management of cubitus varus and valgus. *J Bone Joint Surg* 2005 ; 87-A : 771-80.
13. **Laupattarakasem W, Mahaisavariya B, Kowsuwon W, Saengnipanthkul S.** Pentalateral osteotomy for cubitus varus. Clinical experiences of a new technique. *J Bone Joint Surg* 1989 ; 71-B : 667-70.
14. **Mubarak S WC.** Complications of supracondylar fractures of the elbow. In : Morrey BF, editor. *The elbow and its disorders*. 4th ed, Saunders, Philadelphia, 2009.
15. **Oppenheim WL, Clader TJ, Smith C, Bayer M.** Supracondylar humeral osteotomy for traumatic childhood cubitus varus deformity. *Clin Orthop Relat Res* 1984 ; 188 : 34-9.
16. **Raney EM, Thielen Z, Gregory S, Sobralske M.** Complications of supracondylar osteotomies for cubitus varus. *J Pediatric Orthop* 2012 ; 32 : 232-40.
17. **Sarmiento A, Ebramzadeh E, Brys D, Tarr R.** Angular deformities and forearm function. *J Orthop Res* 1992 ; 10 : 121-33.
18. **Simanovsky N, Lamdan R, Hiller N, Simanovsky N.** The measurements and standardization of humerocondylar angle in children. *J Pediatr Orthop* 2008 ; 28 : 463-5.
19. **Skaggs DL, Glassman D, Weiss JM, Kay RM.** A new surgical technique for the treatment of supracondylar humerus fracture malunions in children. *J Child Orthop* 2011 ; 5 : 305-12.
20. **Takeyasu Y, Oka K, Miyake J, Kataoka T, Moritomo H, Murase T.** Preoperative, computer simulation-based, three-dimensional corrective osteotomy for cubitus varus deformity with use of a custom-designed surgical device. *J Bone Joint Surg* 2013 ; 95-A : e173.
21. **Tricot M, Tran Duy K, Docquier PL.** 3D-corrective osteotomy using surgical guides for posttraumatic distal humeral deformity. *Acta Orthop Belg* 2012 ; 78 : 538-42.
22. **Usui M, Ishii S, Miyano S, Narita H, Kura H.** Three-dimensional corrective osteotomy for treatment of cubitus varus after supracondylar fracture of the humerus in children. *J Shoulder Elbow Surg* 1995 ; 4(1 Pt 1) : 17-22.
23. **Voss FR, Kasser JR, Trepman E, Simmons E, Jr., Hall JE.** Uniplanar supracondylar humeral osteotomy with preset Kirschner wires for posttraumatic cubitus varus. *J Pediatr Orthop* 1994 ; 14 : 471-8.

24. Wright JG, Treble N, Feinstein AR. Measurement of lower limb alignment using long radiographs. *J Bone Joint Surg* 1991 ; 73-B : 721-3.

25. Yamamoto I, Ishii S, Usui M, Ogino T, Kaneda K. Cubitus varus deformity following supracondylar fracture of the

humerus. A method for measuring rotational deformity. *Clin Orthop Relat Res* 1985, 201 : 179-85.

26. Zhang YZ, Lu S, Chen B, Zhao JM, Liu R, Pei GX. Application of computer-aided design osteotomy template for treatment of cubitus varus deformity in teenagers : a pilot study. *J Shoulder Elbow Surg* 2011 ; 20 : 51-6.